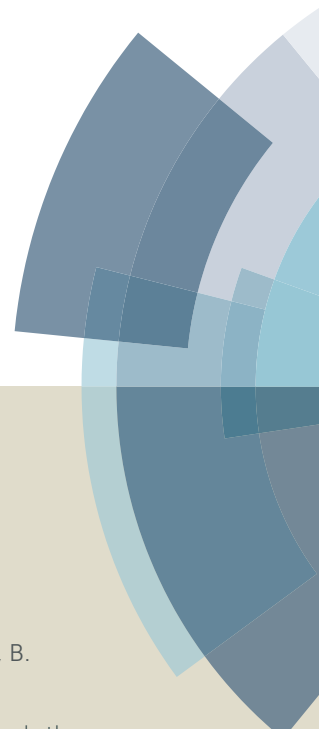
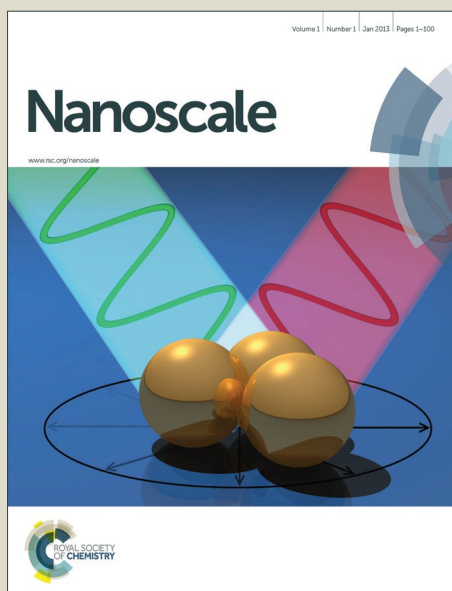


Nanoscale

Accepted Manuscript



This article can be cited before page numbers have been issued, to do this please use: W. Deng, L. Jin, B. Zhang, Y. Chen, L. Mao, H. Zhang and Y. Weiqing, *Nanoscale*, 2016, DOI: 10.1039/C6NR04057H.



This is an *Accepted Manuscript*, which has been through the Royal Society of Chemistry peer review process and has been accepted for publication.

Accepted Manuscripts are published online shortly after acceptance, before technical editing, formatting and proof reading. Using this free service, authors can make their results available to the community, in citable form, before we publish the edited article. We will replace this *Accepted Manuscript* with the edited and formatted *Advance Article* as soon as it is available.

You can find more information about *Accepted Manuscripts* in the [Information for Authors](#).

Please note that technical editing may introduce minor changes to the text and/or graphics, which may alter content. The journal's standard [Terms & Conditions](#) and the [Ethical guidelines](#) still apply. In no event shall the Royal Society of Chemistry be held responsible for any errors or omissions in this *Accepted Manuscript* or any consequences arising from the use of any information it contains.

Flexible Field-Limited Ordered ZnO Nanorods-based Self-Powered Tactile Sensor Array for Electronic Skin

Received 00th January 20xx,
Accepted 00th January 20xx

W. Deng,^a L. Jin,^a B. Zhang,^a Y. Chen,^b L. Mao,^b H. Zhang,^a and W. Yang^{a,*}

DOI: 10.1039/x0xx00000x

www.rsc.org/

Tactile sensor is an essential component for realizing biomimetic robots, while the flexibility of the tactile sensor is a pivotal performance for its application, especially for electronic skin. In this work, a flexible self-powered tactile sensor array was designed based on the piezoelectricity of ZnO nanorods (NRs). The field-limited ordered ZnO NRs were synthesized on flexible Kapton substrate to serve as the function layer of tactile sensor. The electrical output performances of as-fabricated tactile sensor were measured under pressing and bending forces. Moreover, we measured the human-finger pressure detection performance of tactile sensor array, suggesting that the corresponding mapping figure of finger pressure could be displayed on the monitor of personal computer (PC) in the forms of lighted LED and color density through LabVIEW system. This as-grown sensory feedback system should be a potential valuable assistance for the users of hand prostheses to reduce the risk and obtain a greater feeling of using of the prostheses.

Introduction

With the rapid progress of biomimetic robot technology, tactile sensors receive significant attention in the field of electronic skin (*e*-skin)¹. Tactile sensor is an essential device for realizing biomimetic robots^{2,3}. Such a sensor provides data on the shape, position, and force distribution of a contacting stimulus. Unlike industrial robots, a humanoid robot is expected to reach its goal while adapting to the changes in its environment, which requires autonomous learning and safe interaction⁴. In this case, the flexibility of the tactile sensor directly determines its application, especially for *e*-skin⁵⁻⁷. Over the last decade, with the development of related technology⁸⁻¹⁴, tactile sensors with improved performance have been continuously developed based on different physical transduction mechanisms, including piezoresistivity^{15, 16}, capacitance^{17, 18}, triboelectricity¹⁹⁻²², and piezoelectricity^{23, 24}. Among these sensors, piezoelectric sensors present an advantage of no power is necessary²⁵, and this advantage will be more obvious when the large area sensor network is working. In the aspect of application, tactile sensors have been widely explored for use in pressure sensing²⁶, sitting posture classification²⁷, health monitoring²⁸, gait analysis²⁹, and so on.

As a key part of tactile sensor, the selection of functional material is very important for the high-performance *e*-skin. The selected materials must meet the similar mechanical properties to human skin as well as durability to avoid damage from repeated external impacts. Also, they should have good

piezoelectric properties to ensure that they could function as a self-sensing tactile device²⁵. Recently, various nanomaterials, including nanowires³⁰⁻³², carbon nanotubes^{33, 34}, polymer nanofibers^{35, 36}, metal nanoparticles^{37, 38}, graphene^{39, 40}, and many other hybrid materials^{41, 42} have been used for the design of novel tactile sensors. Among the most investigated piezoelectric materials, ZnO NRs deposited on soft substrates have received good attention because of their excellent properties such as good dielectric and piezoelectric properties, low cost hydrothermal synthesis, and no sintering.

In this work, we presented a self-powered tactile sensor array that does not need an external power source for converting the applied pressure into measurable voltage. The key function material of this design is the field-limited ordered ZnO NRs, which grew on the flexible Kapton substrate through a low temperature hydrothermal method. The whole device was packaged with PDMS (polydimethylsiloxane), resulting in a one-piece flexible tactile pressure sensing "skin" that can be draped over the robot surface or prostheses to perceive the variousness of the external force. Combined with the sensory feedback, it can be used for tactile control and display, which could reduce the risk of users not wearing and using their prosthetic hands⁴³.

Experimental Details

The brief fabrication process and the final device structure of the ZnO NRs-based tactile sensor array were shown in Fig. 1.

^a Key Laboratory of Advanced Technologies of Materials (Ministry of Education), School of Materials Science and Engineering, Southwest Jiaotong University, Chengdu 610031, China. E-mail: wayang@swjtu.edu.cn

^b School of Mechanical Engineering, Southwest Jiaotong University, Chengdu 610031, China.

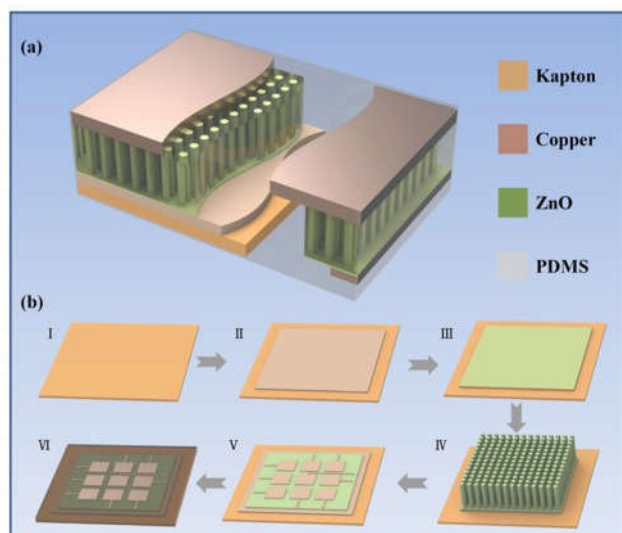


Fig. 1 The schematic illustration of the ZnO NRs-based tactile sensor. The sketch image of flexible self-powered tactile sensor (a); Brief fabrication process of the ZnO NRs-based tactile sensor array (b): (I) The Kapton foil served as the substrate of the tactile sensor. (II) A square copper film was deposited on the substrate served as the bottom electrode of the sensor. (III) A layer of ZnO seed was deposited on the bottom electrode for the synthesis of ZnO NRs. (IV) The ZnO NRs were synthesized via hydrothermal method. (V) The top electrodes array was fabricated through depositing another copper film with the mask to keep the shape and size of every electrode in the same. (VI) The whole device was packaged with the PDMS.

The fabricated tactile sensor was constructed by substrate, piezoelectric layer, top and bottom electrodes and package shell. Kapton foil with a thickness of about 50 μm was selected as the substrate due to its excellent flexibility, high temperature resistance and chemical stability, which has extensively usage in flexible wearable electronic devices⁴⁴. The sketch image and the corresponding fabrication process of the ZnO NRs-based tactile sensor array were illustrated in Fig. 1. First, a square copper film with the thickness of about 300 nm, served as the bottom electrode, was deposited on the central rectangular area of Kapton foil through evaporation technique. Then, a ZnO film with the thickness of about 100 nm, was deposited on the fabricated bottom electrode successively as a seed layer by RF-magnetron sputtering. Next, ZnO NRs were synthesized via a low temperature hydrothermal method⁴⁵. The nutrient solution used in the chemical growth process of ZnO NRs was an aqueous solution of $\text{Zn}(\text{NO}_3)_2 \cdot 6\text{H}_2\text{O}$ and hexamethylenetetramine (HMTA), and the concentration was 0.075 M, which was carried out in a convection oven at 85 $^\circ\text{C}$ for 6 hours. After that, a thin layer of PMMA (polymethyl methacrylate) was spin coated on the surfaces of the substrate at the speed of 3000 rpm, followed by a copper layer deposited on the central area with the mask of electrodes array to ensure every top electrode had the same square shape and size of 1 \times 1 cm. Finally, the whole device was fully packaged with PDMS to provide mechanical support, moisture and dust resistance and allow the sensor

array to be draped conformably over non-planar surfaces. The tactile sensor array was assembled of 3×3 units with the whole size of about 5 \times 5 cm as shown in Fig. 1 (VI).

Results and Discussion

To obtain a more quantitative understanding of the ZnO piezoelectric material, in this paper, we simulated the piezoelectric properties of ZnO NRs through finite element method (FEM)⁴⁶ according to the unique feature of the as-synthesized ZnO NRs.

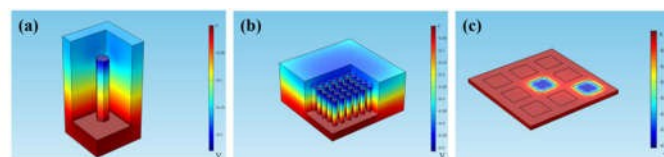


Fig. 2 FEM simulation results of the electric potential distribution generated by various ZnO NR matrix surrounded by air. The voltage mappings of individual (a) and 8×8 matrix (b) ZnO NRs under external force. The voltage mapping of the tactile sensor with 3×3 units, when there were two different units under external forces (c).

In the simulation, the shape of ZnO NR was regular hexagonal prism with diameter of 100 nm and length of 600 nm, which was different from other literatures of cylinder⁴⁷. The simulated structure was surrounded by air, and the ZnO NR contacted with top and bottom electrode. The bottom electrode was fixed and grounded, and the top electrode was rigid with floating potential as boundary conditions. At the same time, a pressure of 1 MPa was applied on the top of one unit. The voltage mapping of individual ZnO NR under external force was shown in Fig. 2 (a). From the results, it is obvious that there are two different electric potentials generated by the ZnO NR under the external force. And the voltage between the electrodes is about 20 mV. When the quantity of the ZnO NRs increases to 64, the electric potential is up to 50 mV as shown in Fig. 2 (b). Fig. 2 (c) shows the distribution of the electric potential generated by NRs array assembled of 3×3 units with two random units under external forces, and without taking into account edge effect and dielectric losses⁴⁸. Obviously, the electric potential of the unit appears in the region of external pressure, and quickly attenuated to be zero beyond the force area, which is wholly independent of each other, and has little influence on the adjacent units, evidently indicating that this NR-based piezoelectric array could be used for tactile sensing without interference among adjacent units.

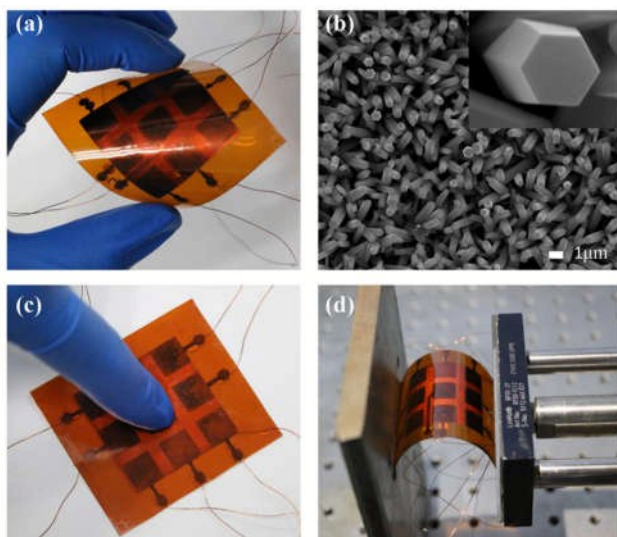


Fig. 3 Photograph of the device, exhibiting the flexibility feature (a). SEM image of ZnO NRs (b). The inset is a vertical view high-magnification image of individual ZnO NR. Pressing (c) and bending (d) measurement of the tactile sensor.

As shown in Fig. 3 (a), the fabricated tactile sensor is bendable due to the intrinsic flexibility of both Kapton foil and PDMS film. Every sensor unit has an independent top electrode and shares the same bottom electrode to construct different electrode couple for electrical signal output. Furthermore, Fig. 3 (b) presents the SEM images of the typical ZnO NRs synthesized on Kapton foil via hydrothermal method. The NRs form a field-limited ordered and dense coverage over the surface of the substrate. The inset is a vertical view high-magnification image, obviously presenting a regular hexagonal cross-section of ZnO NR with a diameter of 50~300 nm. In order to investigate the electrical output performance of as-fabricated tactile sensor, the external mechanical pressing and bending forces were applied through a programmable linear motor, meanwhile, a programmable multimeter and picoammeter were used to detect the electrical output. The typical electrical output characteristics of the tactile sensor array are presented in Fig. 4.

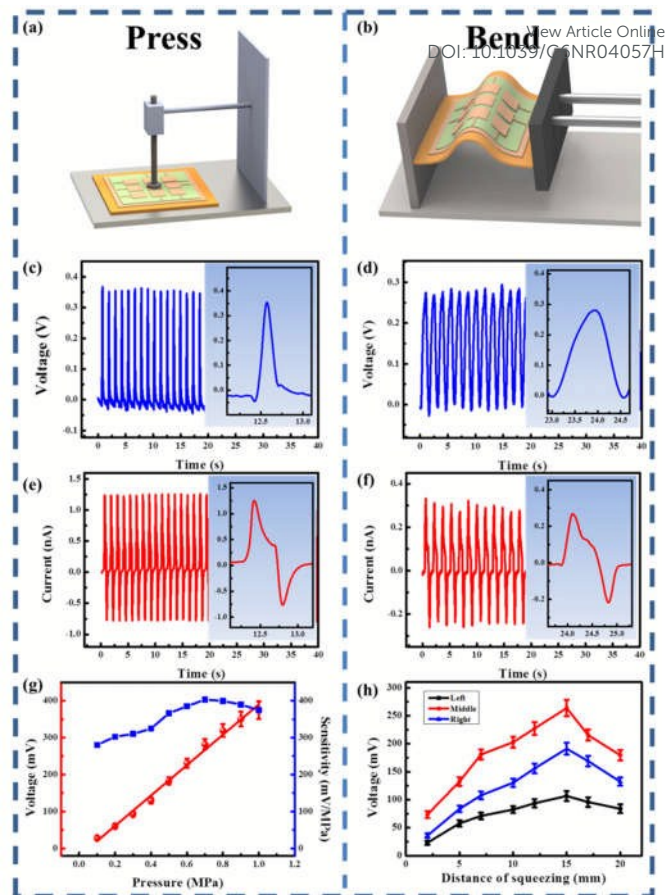


Fig. 4 The schematic diagrams of the pressing (a) and bending (b) measurement. The open-circuit output voltages with the sensors been pressed (c) and bended (d) as a function of time. Inset: enlarged view of one cycle. Short-circuit output currents with the sensors been pressed (e) and bended (f). Inset: enlarged view of one cycle. Voltage response of a single tactile sensor unit as a function of a normal load (with linear fitting) and the sensitivity of the sensor (g). The output voltages of different units as a function of squeezing distances (h).

When the external load of about 1MPa collided with one unit of the sensor array (Fig. 4a), the open-circuit voltages V_{OC} of about 0.35 V (Fig. 4c) were observed ascribing to the slight deformation of the NRs, accompanying with the short-circuit currents I_{SC} of about 1.2 nA (Fig. 4e), which represented the typical electrical output of the tactile sensor in pressing mode. When different forces applied on the tactile sensor array, the voltage response is shown in Fig. 4 (g). The red line is linear fitting curve, which indicates the sensor has good linearity in the measurement range for pressure detecting. The blue curve is the sensitivity of the sensor array. From these results, it is easy to find that the sensitivity of the sensor is not a constant, which is first increased and then decreased along with the increase of external pressure, and the tactile sensor has the best sensitivity of about 403 mV/MPa at 0.7 MPa. That is mainly because the whole device was packaged with PDMS. Some force will be losted in PDMS film when external pressure was applied. The bigger loss, the lower sensitivity. On the other hand, the output of ZnO NRs is not absolute linear with

the external pressure. When the pressure exceeds a certain value, the sensitivity will decrease too. From the results, it is obvious that the fabricated tactile sensor has the best response performance when the external force was near around 0.7MPa.

In addition, our tactile sensor can simultaneously be used to detect the bending forces. The fabricated sensors were studied by a cyclical bending test (Fig. 4b), in which the tactile sensor array is attached to a linear motor moving back and forth, and the relative displacement can be controlled through the program of linear motor. The typical response curves of the fabricated sensor at squeezing distance of 15mm are presented in Fig. 4 (d, f). The V_{OC} of about 0.27 V and the I_{SC} of about 0.3 nA were detected in the experiments. To further study the response of the bending motion, the output voltage of different units were measured as shown in Fig. 4 (h). The units near the linear motor rod are defined as Right units, the other two columns are defined as Middle and Left units respectively, presenting in Fig. 4 (b). From the results, the Middle units have the biggest output voltage among three columns at the same squeezing distance, because the Middle units have bigger deformation than the other two columns under the same condition. Due to the asymmetric deformation of the fixed left end and the right moving end, the output voltage of Left units was smaller than that of Right units. The voltage outputs of all units varied with the degree of bending in the whole measure range, which indicated that this characteristic may be used to detect the degree of bending and determine the position of the unit with the biggest deformation. Furthermore, the response curves of both the pressing and bending forces have high signal-to-noise ratios. Also, this device exhibits good repeatability and stability in response to various external forces.

To demonstrate the potential applications of the tactile sensor array, the as-fabricated tactile sensor can be utilized as a self-powered sensor for monitoring the local touching actions of human fingers or prosthetic hands through data acquisition (DAQ) and LabVIEW system.

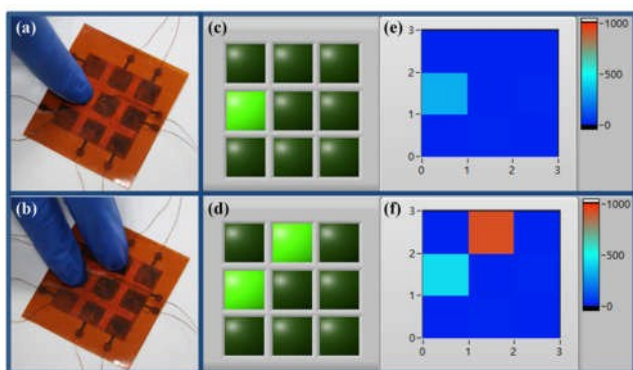


Fig. 5 The as-fabricated tactile sensor array acted as a self-powered sensor for monitoring the local touching actions of human fingers. Photographs of one (a) random tactile sensor unit and two (b) random units touched by human fingers. The

tactile sensors as touch switch (c, d) and quantitative tactile sensitivity (e, f) were displayed in the form of lighted LED and color density, respectively.

The as-fabricated tactile sensor array was fixed on the object, and the electric output of every unit was connected to a PC through DAQ system. When the tactile sensor was touched, the output voltage of the tactile sensor array will be acquired, and the data will be sent to PC for post processing and display. When a random unit in the matrix was pressed (Fig. 5a), a positive voltage signal will be observed. At the same time, the corresponding mapping figure was displayed on the front panel of LabVIEW in the form of lighted LED, as shown in Fig. 5 (c). When two random units were pressed simultaneously (Fig. 5b), both a real-time mapping figures were displayed (Fig. 5 d), which could be used to detect the touch action and served as touch switch. Furthermore, because the voltage output varies with the change of external pressure, it could also serve as pressure sensitivity to detect the touch action and display the relative strength of touch force in the form of color density as shown in Fig. 5 (e,f). On this basis, the as-fabricated tactile sensor array can be realized multi-point touch control through a multi-channel DAQ system, evidently demonstrating the promising applications for the large area display based pressure and bending response.

Conclusions

In summary, we have successfully fabricated a self-powered tactile sensor array based on the piezoelectricity property of field-limited ordered ZnO NRs. The fabricated device exhibited good linearity and flexibility in response to various external forces during pressing and bending experiments. The pressing experiment indicates that the sensor has good linearity in the measurement range and has the best sensitivity of about 403 mV/MPa when the external pressure is near around 0.7 MPa. And the biggest output voltage of about 0.27V was detected in the bending testing when the squeezing distance was 15 mm. The application experiments suggested that the fabricated tactile sensor could serve not only as touch switch but also pressure sensitivity to detect the touch action, and the mapping figure of finger pressure on the tactile sensor could be displayed on PC monitor in the form of lighted LED or color density. Moreover, it could further realize large-area multi-point touch control and display through a multi-channel DAQ system. The demonstrated sensory feedback system may be a valuable assistance for the users of hand prostheses to reduce the risk and obtain a greater feeling of using of the prostheses.

Acknowledgements

This work is supported by Sichuan Province Science and Technology Plan Project (No. 2015JQ0013), the Fundamental Research Funds for the Central Universities (A0920502051408) and the National University Student Innovation Program (201510613009) of China.

Notes and references

- 1 M. L. Hammock, A. Chortos, B. C. Tee, J. B. Tok and Z. Bao, *Adv. Mater.*, 2013, **25**, 5997-6038.
- 2 K.-H. Yu, T.-G. Kwon, M.-J. Yun and S.-C. Lee, *KSME Int. J.*, 2002, **16**, 1222-1228.
- 3 B. P. Nabar, Z. Celik-Butler, D. P. Butler, *IEEE Sens. J.*, 2013, 1-4.
- 4 R. S. Dahiya, G. Metta, M. Valle and G. Sandini, *IEEE T. Robot.*, 2010, **26**, 1-20.
- 5 L. Sangmin, B. Sung-Hwan, L. Lin, Y. Yang, P. Chan, K. Sang-Woo, C. S. Nam, K. Hyunjin, P. Y. Jun, Z. L. Wang, *Adv. Funct. Mater.*, 2013, **23**, 2445-2449.
- 6 B. P. Nabar, Z. Celik-Butler, D. P. Butler, *IEEE Sens. J.*, 2015, **15**, 63-70.
- 7 X. Xiao, L. Yuan, J. Zhong, T. Ding, Y. Liu, Z. Cai, Y. Rong, H. Han, J. Zhou, Z. L. Wang, *Adv. Mater.* 2011, **23**, 5440-5444.
- 8 W. Yang, J. Chen, G. Zhu, J. Yang, P. Bai, Y. Su, Q. Jing, X. Cao and Z. L. Wang, *ACS Nano*, 2013, **7**, 11317-11324.
- 9 W. Yang, J. Chen, Q. Jing, J. Yang, X. Wen, Y. Su, G. Zhu, P. Bai and Z. L. Wang, *Adv. Funct. Mater.*, 2014, **24**, 4090-4096.
- 10 L. Zhang, L. Jin, B. Zhang, W. Deng, H. Pan, J. Tang, M. Zhu and W. Yang, *Nano Energy*, 2015, **16**, 516-523.
- 11 L. Zhang, B. Zhang, J. Chen, L. Jin, W. Deng, J. Tang, H. Zhang, H. Pan, M. Zhu, W. Yang and Z. L. Wang, *Adv. Mater.*, 2016, **28**, 1650-1656.
- 12 Z. L. Wang, J. Chen and L. Lin, *Energy Environ. Sci.*, 2015, **8**, 2250-2282.
- 13 B. P. Nabar, Z. Celik-Butler, D. P. Butler, *IEEE Sens. J.*, 2012, **3**, 1-4.
- 14 S. Zhang, Y. Shen, H. Fang, S. Xu, J. Song, Z. L. Wang, *J. Mater. Chem.* 2010, **20**, 213-222.
- 15 C. L. Choong, M. B. Shim, B. S. Lee, S. Jeon, D. S. Ko, T. H. Kang, J. Bae, S. H. Lee, K. E. Byun, J. Im, Y. J. Jeong, C. E. Park, J. J. Park and U. I. Chung, *Adv. Mater.*, 2014, **26**, 3451-3458.
- 16 H. Tian, Y. Shu, X. F. Wang, M. A. Mohammad, Z. Bie, Q. Y. Xie, C. Li, W. T. Mi, Y. Yang and T. L. Ren, *Sci. Rep.*, 2015, **5**, 8603.
- 17 X. Guo, Y. Huang, X. Cai, C. Liu and P. Liu, *Meas. Sci. Technol.*, 2016, **27**, 045105.
- 18 W. Deng, X. Huang, W. Chu, Y. Chen, L. Mao, Q. Tang and W. Yang, *J. Sens.*, 2016, **2016**, 8.
- 19 Y. Yang, H. Zhang, Z.-H. Lin, Y. S. Zhou, Q. Jing, Y. Su, J. Yang, J. Chen, C. Hu and Z. L. Wang, *ACS Nano*, 2013, **7**, 9213-9222.
- 20 W. Yang, J. Chen, X. Wen, Q. Jing, J. Yang, Y. Su, G. Zhu, W. Wu and Z. L. Wang, *ACS Appl. Mater. Interfaces*, 2014, **6**, 7479-7484.
- 21 G. Zhu, W. Q. Yang, T. Zhang, Q. Jing, J. Chen, Y. S. Zhou, P. Bai and Z. L. Wang, *Nano Lett.*, 2014, **14**, 3208-3213.
- 22 J. Chen, G. Zhu, J. Yang, Q. Jing, P. Bai, W. Yang, X. Qi, Y. Su and Z. L. Wang, *ACS Nano*, 2015, **9**, 105-116.
- 23 C. Pan, L. Dong, G. Zhu, S. Niu, R. Yu, Q. Yang, Y. Liu and Z. L. Wang, *Nat. Photonics*, 2013, **7**, 752-758.
- 24 İ. Murat Koç and E. Akça, *Tribol. Int.*, 2013, **59**, 321-331.
- 25 S. K. Hwang and H. Y. Hwang, *Smart Mater. Struct.*, 2013, **22**, 055004.
- 26 Y. Hu, C. Xu, Y. Zhang, L. Lin, R. L. Snyder, Z. L. Wang, *Adv. Mater.* 2011, **23**, 4068-4071.
- 27 J. Meyer, B. Arnrich, J. Schumm and G. Tröster, *IEEE Sens. J.*, 2010, **10**, 1391-1398.
- 28 X. Wang, Y. Gu, Z. Xiong, Z. Cui and T. Zhang, *Adv. Mater.*, 2014, **26**, 1336-1342.
- 29 L. Shu, T. Hua, Y. Wang, Q. Li, D. D. Feng and X. Tao, *IEEE T. Inf. Technol. B.*, 2010, **14**, 767-775.
- 30 Z. L. Wang, *Appl. Phys. A: Mater. Sci. Process.*, 2007, **88**, 7-15.
- 31 M. Ha, S. Lim, J. Park, D.-S. Um, Y. Lee and H. Ko, *Adv. Funct. Mater.*, 2015, **25**, 2841-2849.
- 32 Y. Jeong, M. Sim, J. H. Shin, J.-W. Choi, J. I. Sohn, S. N. Cha, H. Choi, C. Moon, J. E. Jang, *RSC Adv.* 2015, **5**, 40363-40368.
- 33 T. Yamada, Y. Hayamizu, Y. Yamamoto, Y. Yomogida, A. Izadi-Najafabadi, D. N. Futaba and K. Hata, *Nat. Nanotechnol.*, 2011, **6**, 296-301.
- 34 D. J. Cohen, D. Mitra, K. Peterson and M. M. Maharbiz, *Nano Lett.*, 2012, **12**, 1821-1825.
- 35 Q. Gao, H. Meguro, S. Okamoto and M. Kimura, *Langmuir*, 2012, **28**, 17593-17596.
- 36 C. Pang, G.-Y. Lee, T.-i. Kim, S. M. Kim, H. N. Kim, S.-H. Ahn and K.-Y. Suh, *Nat. Mater.*, 2012, **11**, 795-801.
- 37 M. Segev-Bar, A. Landman, M. Nir-Shapira, G. Shuster and H. Haick, *ACS Appl. Mater. Interfaces*, 2013, **5**, 5531-5541.
- 38 N. M. Sangeetha, N. Decorde, B. Viallet, G. Viau and L. Ressler, *J. Phys. Chem. C*, 2013, **117**, 1935-1940.
- 39 H. B. Yao, J. Ge, C. F. Wang, X. Wang, W. Hu, Z. J. Zheng, Y. Ni and S. H. Yu, *Adv. Mater.*, 2013, **25**, 6692-6698.
- 40 C. Dukhyun, C. Min-Yeol, C. W. Mook, S. Hyeon-Jin, P. Hyun-Kyu, S. Ju-Seok, P. Jongbong, Y. Seon-Mi, C. S. Jin, L. Y. Hee, *Adv. Mater.*, 2010, **22**, 2187-92.
- 41 M. Di Donato, S. Bocchini, G. Canavese, V. Cauda and M. Lombardi, *Key Eng. Mater.*, 2014, **605**, 263-266.
- 42 H. Hwang, *Mech. Compos. Mater.*, 2011, **47**, 137-144.
- 43 C. Antfolk, C. Balkenius, G. Lundborg, B. Rosén and F. Sebelius, *J. Med. Biol. Eng.*, 2010, **30**, 355-360.
- 44 P. Bai, G. Zhu, Y. S. Zhou, S. Wang, J. Ma, G. Zhang and Z. L. Wang, *Nano Res.*, 2014, **7**, 990-997.
- 45 Y. Hu, Y. Zhang, C. Xu, L. Lin, R. L. Snyder and Z. L. Wang, *Nano Lett.*, 2011, **11**, 2572-2577.
- 46 R. Tao, G. Ardila, L. Montès and M. Mouis, *Nano Energy*, 2015, **14**, 62-76.
- 47 R. Araneo and C. Falconi, *Nanotechnol.*, 2013, **24**, 265707.
- 48 R. Hinchet, S. Lee, G. Ardila, L. Montès, M. Mouis and Z. L. Wang, *Adv. Funct. Mater.*, 2014, **24**, 971-977.